1 Brief

This report consists of three tasks in Barcelona. Task 1 involves the replacement of R12 fluid with environment-friendly refrigerants in either single or cascade vapour compression system. It is concluded that employing solely R134a in cascade system yields a nearly equivalent COP as R12 and is regarded as the best substitute. Task 2 is associated with the air-conditioning system modifications, the initial system is not capable of maintaining a constant room temperature of 13°C which is proposed to be altered by either modulating the water flow rate or air flow. The water-modulate scenario represents the best system modification to achieve a steady air temperature with the minimum energy consumption. In contrast, the air-control case requires much more energy to operate since the quantity of air blown into the room is much higher than the nominal flow rate. Therefore, the fan operates heavily demanding high energy consumption and potentially leads to chiller over-loading. Bringing down the water flow rate can reduce the amount of air blown hence lowering the fan energy. Task 3 concerns building a PV plant to offset the energy requirement of the air-conditioning system. Optimal PV panels' azimuth angle and tilt angle are found to be 0° due south and 26.4° respectively, which is employed to maximise the solar radiation and calculate the panel area requirement. It is concluded that almost 3800m^2 panels are necessary to fully offset the energy consumption in the water-modulate case which in impractical. Further improvements can concentrate on purchasing higher efficiency PV panels to enlarge the quantity of electricity generated or design integrated system to reduce the energy requirements, such as the PV/T and BIPV.

2 Project 1

2.1 Introduction

R12 is now considered as a culprit for the ozone depletion due to the excessive greenhouse effect. The Montreal Protocol has legally claimed the phase-out of R12 before 2021 (Khemani, 2011). The client proposed upgrading plans to either change the R12 with its alternatives R404A and R134a or employ the cascade system with different refrigerant combinations. Methodologies of how to calculate the COP for both scenarios is presented. The results are analysed and discussed with the best approach proposed by considering the financial and environmental aspects. Finally, the analysis constraints are highlighted for further work.

2.2 Methodology and assumptions

CoolProp package is used throughout to aid the calculation of COP for both upgrade scenarios. In the single stage vapour compression system, the original R12 is simply replaced by more environmentally friendly refrigerant, R404A and R134a. The COP is the ratio between the desired cooling effect and the work required. More explicitly, the desired refrigeration effect is denoted as Q_{41} whereas the required work is done purely by compressor, labelled as W_{12}, hence $COP = \frac{Q_{41}}{W_{12}}$. Concerning the COP and environmental influences, the results of each solution will be comparatively evaluated by referring to the original system with R12.

Scenario 2, composed of 4 sub-cases, employs more advanced cascade vapour compression system. The cascade system consists of two single-stage vapour compression systems working in series, in which the lower temperature cycle produces the refrigeration effect. In fact, the cascade system is more practically used in the industry where the moderately low temperature is necessary, for instance, the frozen food factory. In contrast, the single vapour compression system appears incompetent since it's impractical to create a large temperature difference. Comparing with the single-stage system, the cascade system allows for the use of different combination of fluids in the lower and higher temperature respectively. Rationally selecting different fluids help to optimise the COP and reduce the adverse environmental effect. Furthermore, Fig1 shows that the cascade system attains better efficiency by the reduced work and increased refrigeration effect (Kapadia and Parmar, 2015).

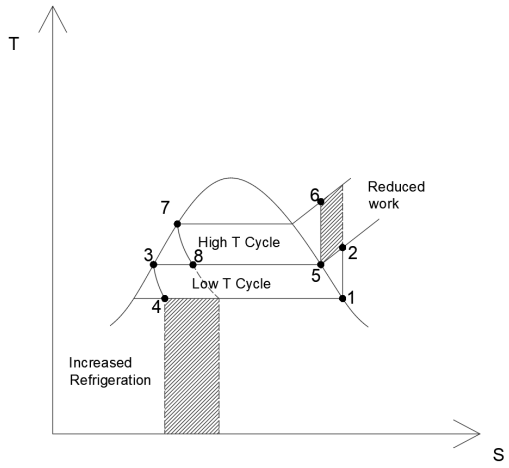

Figure 1-T_S graph for cascade system

4 sub-cases are classified as two categories, case a/b uses the single fluid whereas case c/d uses two different fluids, the subcases are tabulated in Table 1. In terms of the thermodynamic analysis, the crucial difference between these two categories lies in the assumption made for the pressure at the cascading part. In case a/b, the pressure at condenser of low temperature cycle (P_{c_low}) is equivalent to the pressure of the evaporator of high temperature cycle (P_{e_high}). This assumption is no longer tenable in the case c/d. It's also worth noting that by assuming an adiabatic counter flow heat exchanger, $T_{c\_low} \approx T_{e\_high}$. The detailed derivation process is presented below.

The COP is written as:

$$COP = \frac{Q_{41}}{W_{12} + W_{56}}$$

The refrigeration effect is defined:

$$Q_{41} = \dot{m}_{low}\,(h_1 - h_4)$$

Compressor work at lower temperature cycle:

$$W_{12} = \dot{m}_{low}\,(h_2 - h_1)$$

Compressor work at higher temperature cycle:

$$W_{56} = \dot{m}_{high}\,(h_6 - h_5)$$

Given the adiabatic counter flow heat exchanger, the heat rejected by the lower temperature cycle condenser Q_{23} equals to the heat absorbed at the evaporator Q_{85} of the higher temperature cycle. This relationship gets rid of the unknown mass flow rate of two fluids:

$$Q_{23} = -\dot{m}_{low}\,(h_3 - h_2) = \dot{m}_{low}\,(h_2 - h_3)$$

$$Q_{85} = \dot{m}_{high}\,(h_5 - h_8)$$

$$Q_{85} = Q_{23}$$

$$\dot{m}_{low}\,(h_2 - h_3) = \dot{m}_{high}\,(h_5 - h_8)$$

Thus, COP is derived:

$$COP = \frac{\dot{m}_{low}\,(h_1 - h_4)}{\dot{m}_{low}\,(h_2 - h_1) + \dot{m}_{high}\,(h_6 - h_5)} = \frac{\dot{m}_{low}\,(h_1 - h_4)}{\dot{m}_{low}\,(h_2 - h_1) + \frac{\dot{m}_{low}\,(h_2 - h_3)\,(h_6 - h_5)}{(h_5 - h_8)}}$$

$$COP = \frac{(h_1 - h_4)(h_5 - h_8)}{(h_2 - h_1)(h_5 - h_8) + (h_2 - h_3)\,(h_6 - h_5)}$$

The intermediate temperature for all 4 sub-cases is assumed which is then optimised for the highest available COP using Python. The COP is plotted against the intermediate temperature and the system performance is comparatively evaluated and discussed. The more detailed calculation procedures are displayed in the Python files with annotations.

Table 1-System design information

	Lower temperature cycle	Higher temperature cycle	Categories	Assumptions
Case a	R404A	R404A	Sigle fluid	Tc_low = Te_high
Case b	R134a	R134a		Pc_low = Pe_high
Case c	R404A	R134a	Double fluid	Tc_low = Te_high
Case d	R134a	R404A		Pc_low ≠ Pe_high

2.3 Analysis and discussion

The COP is calculated in the upgrading scenario 1, it turns out that the COP of using R404A is 1.68, of using R134a is 2.12 and the COP of original R12 is 2.23. Therefore, in terms of the system performance, the proposed fluid R134a outperforms the R404A. However, both upgrading refrigerants are inferior to the original R12. Under this circumstance, the R134a with the closer COP is considered as the best alternative of R12. Besides, when it comes to the environment saving, the R134a produces very low greenhouse effect leading to no ozone depletion. The results of scenario 2 are tabulated in Table 2.

Table 2-Analysis result for each design option

	Lower temperature cycle	Higher temperature cycle	COP	Intermediate Temperature (K)	Intermediate Temperature (°C)
Case a	R404A	R404A	2.40	289	16
Case b	R134a	R134a	2.69	288	15
Case c	R404A	R134a	2.59	283	10
Case d	R134a	R404A	2.52	295	22
Case R12	R12	R12	2.74	287	14

The case b, where refrigerant R134a is applied to both lower and higher temperature cycles, performs the best among the 4 subcases. Accordingly, Fig 2 illustrates that the case b, highlighted in red has the optimal intermediate temperature of 288K.

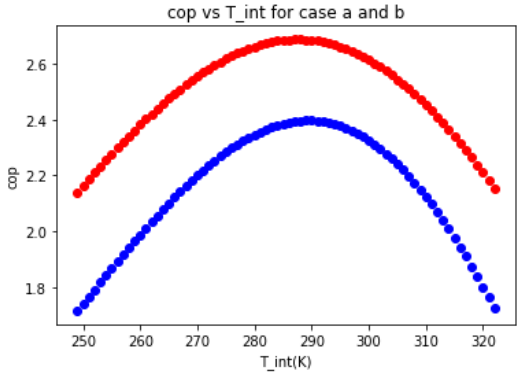

Figure 2-COP for case a/b

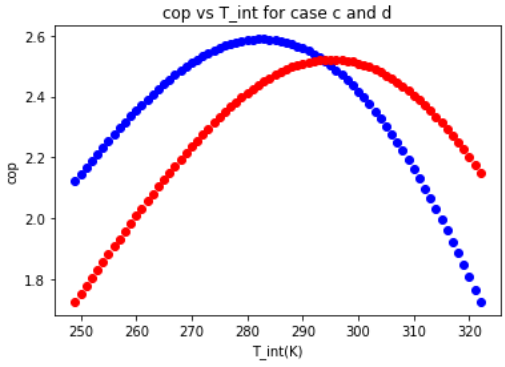

Figure 3-COP for case c/d

Evidently, the case b with COP of 2.69 overtakes the original R12 refrigerant with COP of 2.23 in single system. This outperformance is achieved by employing the cascade system. COP of 2.74 is yielded when R12 is applied to the cascade system, remains the best from the aspect of system performance. Therefore, purely from the COP perspective, $Cascade(R12) > cascade(b) > cascade(c) > cascade(d) > cascade(a) > single(R12) > single(R134a) > single(R404A)$. However, cascade system requires higher capital

investment and it is strongly recommended to employ the case b with cascade system and perform a payback calculation to take account of both finance and the environmental aspects. It's also worth noting that the intermediate temperature is assumed to be the same for all four cases which is rarely true in practice. The pressure drop is neglected and the changes in kinetic and potential energy are also out of consideration. If necessary, further work is required to obtain more accurate results.

3 Project 2

3.1 Introduction

The objective of this task is to find the best option of maintaining constant 13°C with minimum energy consumption. The first modification modulates the water while the second modification focuses on controlling the air flow rate. Along with the base-case, all three models are simulated using Dymola to perform a systematic analysis. Alternative remediation for is proposed and the restraints of the analysis and assumptions are addressed for future studies.

3.2 Methodology and assumptions

Based on the model in the Dymola, the principal energy consumption comprising chiller, pump and fan are calculated. The optimal operation system is selected, purely based on energy consumption during week 34. The pump energy consumption is firstly analysed, followed by a detailed evaluation of chiller energy. The fan energy is also reviewed, and the rationales behind the energy use for each component of all scenario are carefully investigated that cover chiller COP, heat exchange rate, air flow rate in both controlled and uncontrolled cases etc.

3.3 Analysis and discussion

Fig 4,5,6 show that the second modification involving adjusting the air flow rate, consumes the largest quantity of energy to maintain the system operation, namely 2.05×10^{12}J. On the other hand, the water-modulate case uses the least energy 7.2×10^{10}J and the base-case requires 9.3×10^{10}J.

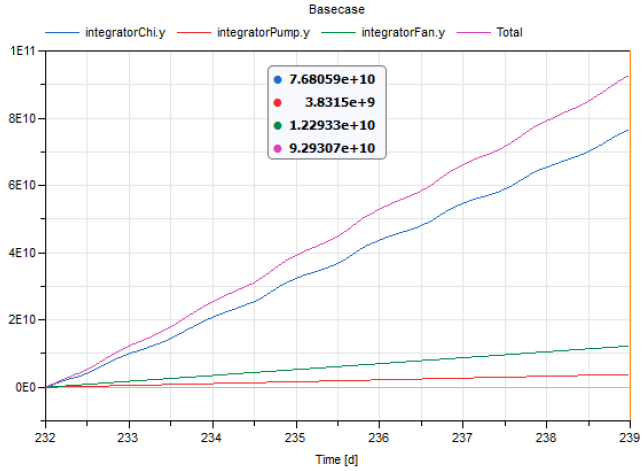

Figure 4-Energy consumption for base case

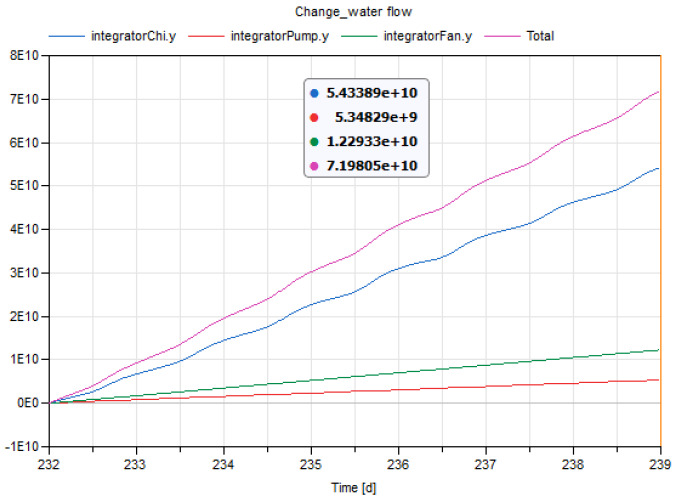

Figure 5-Energy consumption of water-modulate case

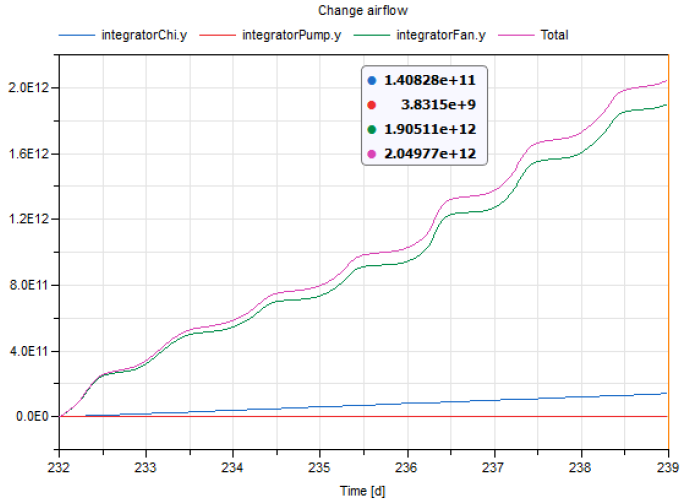

Figure 6-Energy consumption of air-control case

Explicitly, the energy consumption of the water pump remains the same for the base-case and air-control case, since the water flow rate is constant 32kg/s. Oppositely, the water-modulate case has water flow rate continuously varied resulting in high energy requirements. Compared with the base-case, modulating water consumes less energy of the chiller due to the existence of bypass. A portion of redundant water is split directly towards water pump, mixing with the returned water from heat exchanger leading to relatively low temperature. The cooled water requires less chilling power to reach the setpoint 7°C. In contrast, the system with air control has nearly two-fold chiller energy consumption than base-case. This substantial chiller energy arises from the high heat exchange rate and thus high returned water temperature which is evidenced by Fig 7. Heat exchange rate for this modification is considerably higher than base-case and water-modulate case.

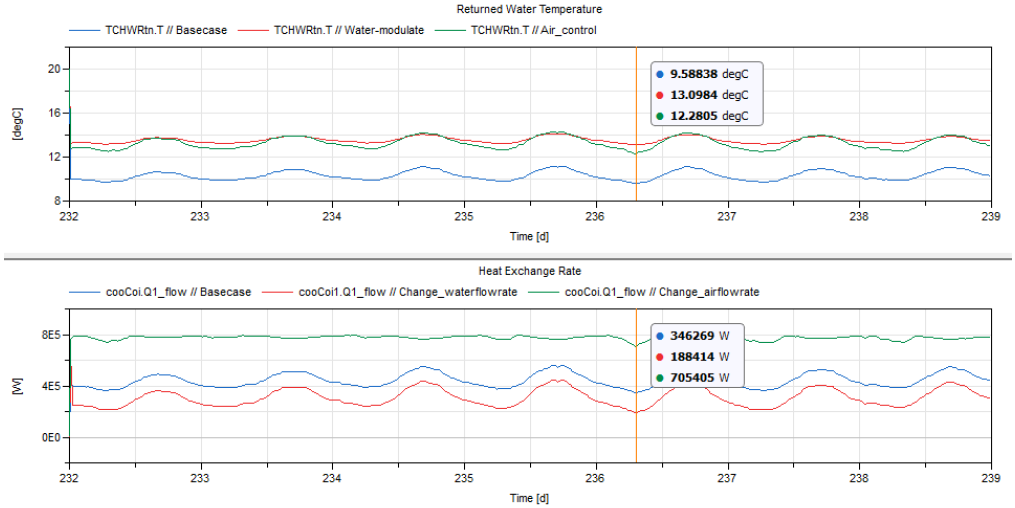

Figure 7-Returned water temperature/Heat exchange rate

Furthermore, there is a close relationship spotted between the amount of heat transfer in the cooling coil, the air flow rate and the outside dry bulb temperature in air-control case, see Fig 8. The lower dry bulb temperature results in higher air flow rate which is due to the goal of achieving 13°C in the room. The outside air with lower temperature or enthalpy needs less energy extraction within the cooling coil, thus the control system delivers the air faster or higher air flow rate to avoid the air being overcooled. The air flow rate ranges from approximately 40kg/s up to 140kg/s. However, the heat exchange rate line is invariably flat indicating that no matter 40kg/s or 140kg/s, the heat exchange rate in the cooling coil has reached the maximum capacity of the chiller because the high air flow rate carries large amount of energy for exchange. Evidently, the heat exchange rate around 750kW matches the pre-set chiller capacity 743.4kW, the chiller operates heavily consuming much more energy than the base-case and water-adjusted case. Additionally, the quantity of air is considerably higher than the nominal air flow rate 16kg/s leading to enormous fan energy consumption in the air-control scenario.

It is worth mentioning that Fig 7 illustrates that the heat exchanged in the base-case has the same pattern as the water-modulate case but slightly more energy transfer. The reason is that the output air temperature is constant 13°C in the water-modulate case while the temperature fluctuates between 8°C-10°C in the base-case. Lower output temperature means more heat is exchanged within the cooling coil, shifting the base-

case up. Moreover, the air-control case has distinct pattern, owing to the limited capacity of chiller. It is unquestionable that increasing the chiller capacity, for instance to 1000kW, the heat exchange pattern can be restored to the same pattern as base-case and water-modulate case. Additionally, provided the constant water flow rate in the base-case and air-control case, higher heat exchange rate causes higher returned water temperature. Although water-modulate case possesses the least energy, the splitter lowering the water flow rate results in higher returned water temperature. The profile of the water-modulate case is different since it's not only affected by the outside temperature, but also the variation of water flow rate.

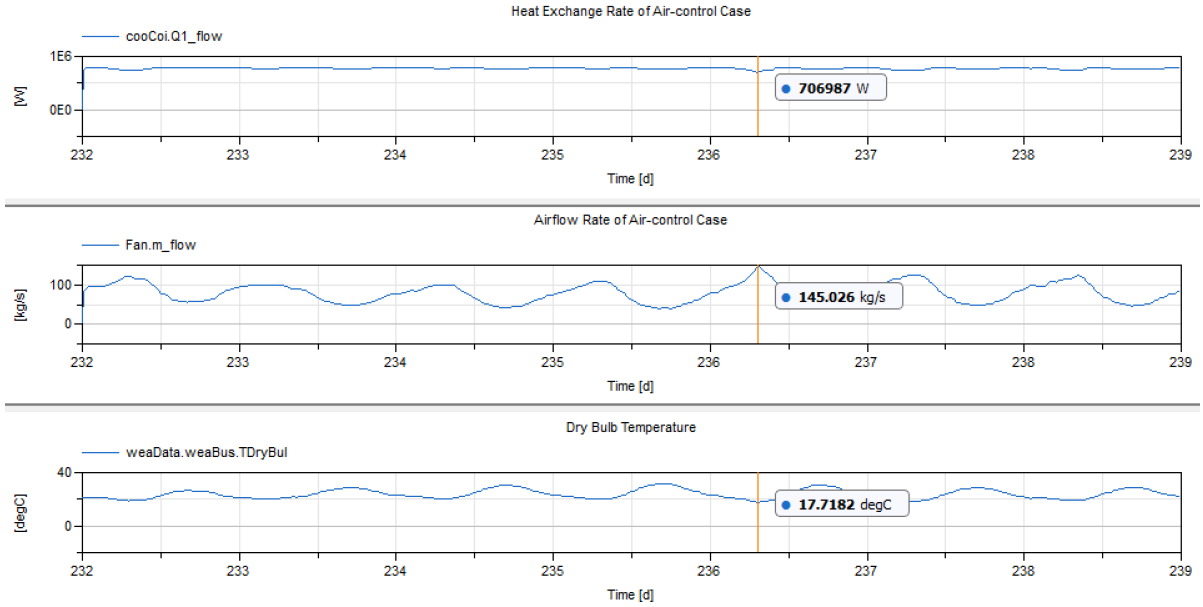

Figure 8-Heat exchange rate/Air flow rate/Dry bulb temperature

It is also highlighted in Fig 8, lower dry bulb temperature with higher air flow rate causes lower heat transfer rate in the cooling coil. As previously explained, lower outside temperature or h_{a2} leads to increase of m_a, the delivered air or h_{b2} is constant and the differences of enthalpy, which is numerically more dominating than m_a, decreases, hence resulting in the Q decreases ($Q=m_a(h_{b2}-h_{a2})$).

In terms of the chiller COP, Fig 9 exhibits that generally lower outside temperature, thus lower inside-outside temperature difference gives rise to higher COP. Base-case and water-modulate case is overlapped while the air-control case has lower COP at low point. This is due to the overloading of the chiller at high dry bulb temperature, the work for compressor keep increasing to some extent while the refrigeration effect has capped to 743.7kW. The t_{ch_out} fluctuates exceeding 7°C occasionally results in lower COP.

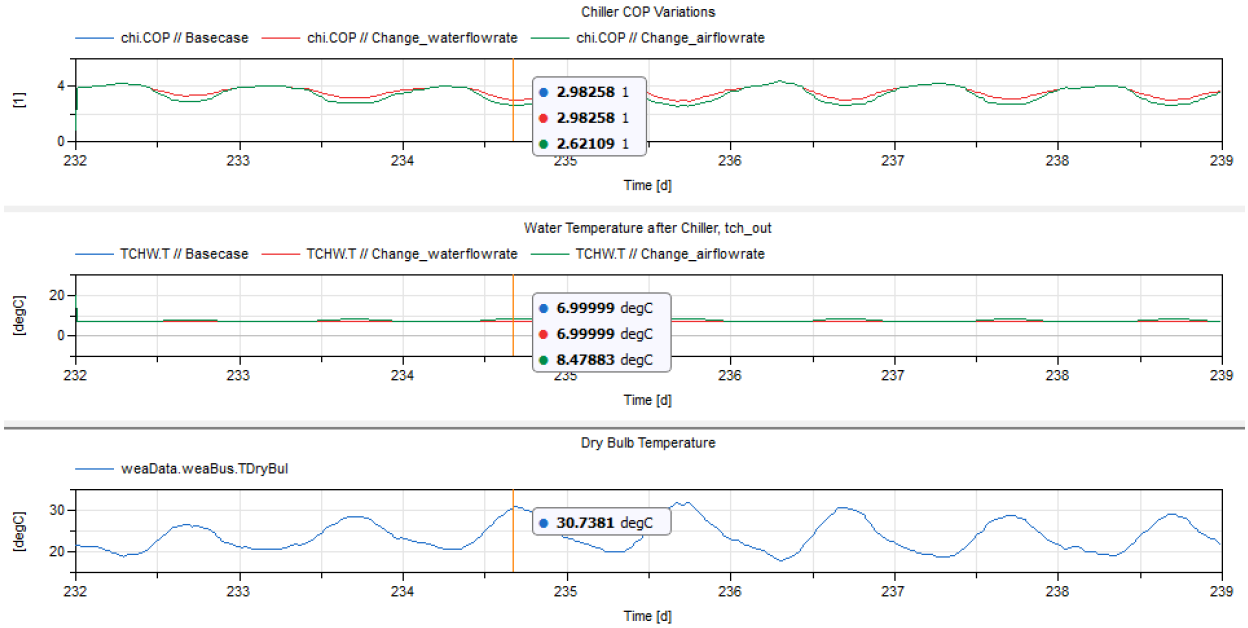

Figure 9-COP variations/tch_out/Dry bulb temperature

Fig 10 demonstrates that less water is split to cool the fixed air flow in the water-modulate case when the outside temperature is low. Therefore, the splitter control mechanism follows the profile of outside temperature.

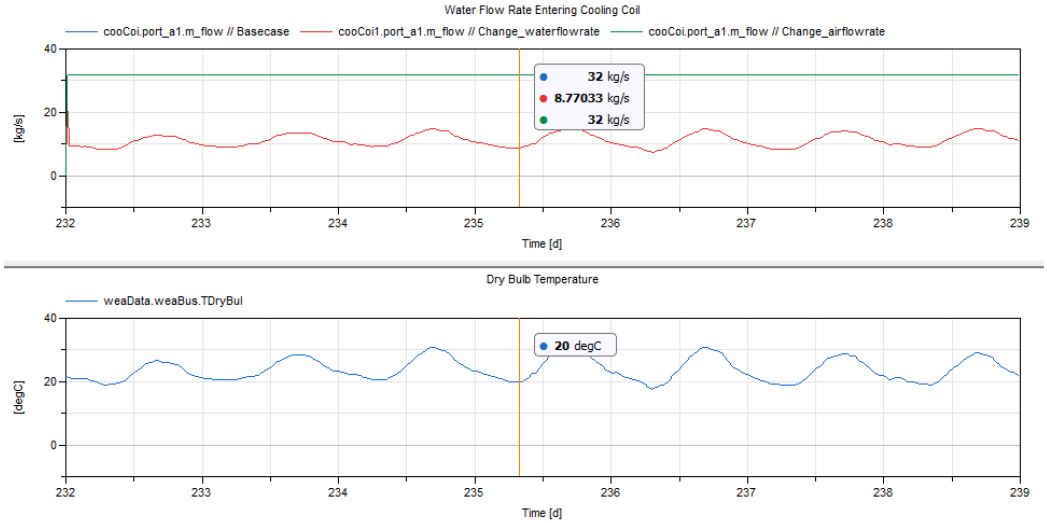

Figure 10-Split water flow/Dry bulb temperature

Fig 11 showcases that PI(proportional-integral) works perfectly to modulate the water, but the marginal fluctuation of air-control case implies that PID(proportional-integral-derivative) control does not work steadily due possibly to the massive air flow rate.

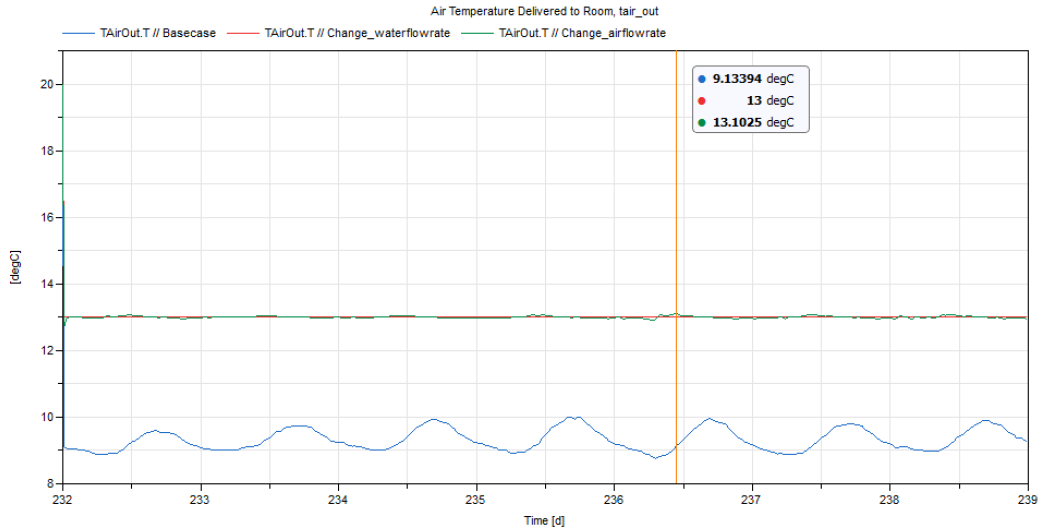

Figure 11-tair_out

It's been proven that the air-control system works more efficiently when the outside temperature is higher with lower air flow rate. Although the chiller energy increases, the pump energy is reduced more significantly leading to overall less energy consumption. Remediation is to reduce the air flow rate by minimising the water flow rate $m_w(h_{b1}-h_{a1})=m_a(h_{b2}-h_{a2})$. The water flow rate is altered from 32kg/s to 1kg/s and the results are shown in Fig 12. The air flow and total energy consumption are considerably lower and the PID copes better. However, the adverse effect is that the air flow is lessened for ventilation. Therefore, the water-case is the best option since we have fixed desired the air flow, modulating the water can reach low energy operation. Alternatively, the air-control case can couple with external ventilation system, the performance remains unknown but worth trying in future studies.

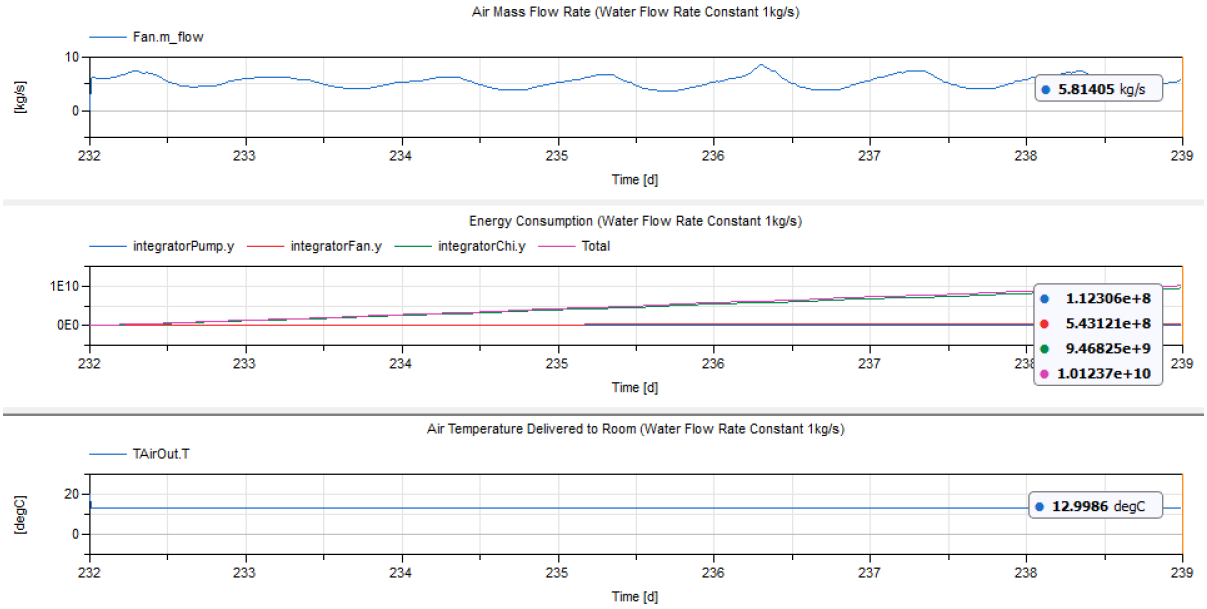

Figure 12-Air flow rate/Energy consumption/Conditioned air temperature (water flow rate constant 1kg/s)

Finally, the fan in base-case and water-control case works with the consideration of air temperature increase due to the fan operation. The air temperature prior to entering the heat exchange increases 1°C. Nonetheless, the fan in the air-control case is set to be ideal which does not account for the air temperature increase. Practically, this assumption is not true since working in heavy load results in great temperature increases and chiller COP drops. More studies are recommended to simulate the system more realistically for genuine energy comparison.

4 Project 3

4.1 Introduction

The objective of this project lies in assessing the potential of employing the PV plant to offset the operational energy of scenario 2, where water flow rate is modulated. The PV azimuth and tilt angle are rationally chosen to calculate the required PV area. The theoretical area is then optimised by taking the PV efficiency and working mechanism into account. The alternative renewable strategy is proposed, and the constraints of the analysis are highlighted.

4.2 Methodology and assumptions

The net surface area, tilt angle and the azimuth angle of PV panels are investigated to achieve the optimally available electricity. Geographically, Barcelona is in the North hemisphere, orienting the PV panels to the South helps to absorb the most solar radiation. In terms of tilt angle, several authors have proposed an optimum tilt angle-latitude relation. Table 3 is collected by Yadav and Chandel, 2013, representing different recommended tilt angles. Additionally, the Spanish Technical Building Code recommends the tilt angle 10° below the local latitude for the PV systems (Girard *et al.*, 2016). By combining these suggestions, the relations of ±10°, ±15° and 20° will be examined to find the best tilt. Provided that local latitude of Barcelona is 41.4°, the tilt angles being examined are 51.4°, 31.4°, 56.4°, 26.4° and 61.4°. Finally, the area of the PV plant is adjusted and determined by covering the power consumed by the fan, pump and chiller from the first modification scenario during week 34. Noting that the fraction of area and conversion efficiency is kept as 0.9 and 0.12 respectively throughout the calculation.

Table 3-Tilt angle-latitude relations (Yadav and Chandel, 2013)

References	Recommended tilt angle	Remarks
Duffie and Beckman [6]	$(\phi+15^\circ)\pm15^\circ$	These methods are suitable for calculating approximate tilt angles for different latitudes. The minus sign is used for summer season and the positive sign for winter season.
Heywood [32]	$\phi-10^\circ$	
Lunde [33]	$\phi\pm15^\circ$	
Chinnery [34]	$\phi+10^\circ$	
Löf and Tybout [35]	$\phi+(10^\circ\rightarrow30^\circ)$	
Garg [36]	$\phi+15^\circ$, $\phi-15^\circ$, 0.9ϕ	
Hottel [37]	$\phi+20^\circ$	
Kern and Harris [38]	$\phi+10^\circ$	
Yellot [39]	$\phi+20^\circ$	
Elminir et al. [40]	$(\phi+15^\circ)\pm15^\circ$	

4.3 Analysis and discussion

By sticking with 100m^2 panel area, the optimal angle (26.4°) is calculated which corresponds to the 15° below the local latitude (see Table 4). It is also observed that 10° higher than the latitude yields very comparable energy. The area required to offset the electricity consumption is determined by using tilt angle 26.4° and 0° for south orientation.

Table 4-Optimal tilt angle selection

	Til_51.4°	Til_31.4°	Til_56.4°	Til_26.4°	Til_61.4°
Total Energy (J) at Week 34	1909849651	1790297689	1731718765	1910032566	1662413479
Ranking	2	3	4	1	5
Percentage	114.88%	107.69%	104.17%	114.90%	100.00%

Fig 5 illustrates that approximately 7.2x10^{10}J is consumed by chiller, pump and fan in scenario 2. The area is adjusted to generate same quantity of energy which indicates 3800m^2 with 7.26x10^{10}J. Unsurprisingly, the area of the panels required is huge that implies a substantial amount of investment to build the massive PV plant. However, this area could be reduced by selecting proper PV panels or tracking mechanisms. 12% conversion efficiency was used to work out the area. Green *et al.*, 2018 regularly reports the latest officially tested PV panels, up to 2018, single junction cell can provide 28.8% conversion efficiency and the multiple-junction can reach 38.8%. These latest PV panels are more expensive due to the advanced technology, performing a payback calculation to choose the most appropriate panels can offer an insight into what the most cost-effective solution is. Additionally, the application of PV/T system could be an alternative to increase the efficiency by reducing the temperature on the panel (Baljit, Chan and Sopian, 2016). Regarding the tilt angle, tracking mechanism enables the panels to track the sun minute by minute, hence enhancing the amount of solar radiation captured. Unquestionably, the tracking mechanism requires regular maintenance and greater capital investment than static panels. Instead of building a PV plant to generate electricity, there is a potential to employ the building integrated PV (BIPV). Properly designed integrated system can reduce the heat transfer through the opaque elements, hence keep inside cool. The integrated PV panels work as shading while collecting solar radiation to generate electricity.

It is worthwhile addressing some constraints that potentially lead to the performance gap between theoretical calculation and practical situation. The efficiency of the PV panel tends to decrease since energy is lost through moss growth, dirt residue or stained glazing (Lo, 2015). These facts could not be analysed by any means in simulation but likely compromise the PV efficiency. Moreover, the entire analysis is performed by considering only the Week 34. The tilt angle can be potentially changed if the annual optimum is evaluated.

5 Reference

Baljit, S. S. S., Chan, H. Y. and Sopian, K. (2016) 'Review of building integrated applications of photovoltaic and solar thermal systems', Journal of Cleaner Production. Elsevier Ltd, 137, p. 678. doi: 10.1016/j.jclepro.2016.07.150.

Girard, A. et al. (2016) 'Spain's energy outlook: A review of PV potential and energy export', Renewable Energy, 86, p. 709. doi: 10.1016/j.renene.2015.08.074.

Green, M. A. et al. (2018) 'Solar cell efficiency tables (version 52)', Progress in Photovoltaics: Research and Applications, 26(7), pp. 427–436. doi: 10.1002/pip.3040.

Kapadia, R. . and Parmar, G. G. (2015) 'Thermodynamic Analysis of Cascade Refrigeration System using a Natural Refrigerants for Supermarket Application', International Journal of Innovative Research in Science, Engineering and Technology, 4(6), pp. 1–8.

Khemani, H. (2011) Replacement for R12 Refrigerant or Freon 12 (R12) Replacement.

Lo, S. (2015) 'Fundamentals of PV and solar thermal technologies (Tutorial)'.

Yadav, A. K. and Chandel, S. S. (2013) 'Tilt angle optimization to maximize incident solar radiation: A review', Renewable and Sustainable Energy Reviews. Elsevier, 23, pp. 503–513. doi: 10.1016/j.rser.2013.02.027.